Pergamon

Journal of Structural Geology, Vol. 16, No. 9, pp. 1243 to 1257, 1994

0191-8141/94 $07.00+0.00

0191-8141(93)E0014-C

Magnetic fabric and structural setting of Plio-Pleistocene clayey units in an extensional regime: the Tyrrhenian margin of central Italy

LEONARDO SAGNOTTI

Istituto Nazionale di Geofisica, Via di Vigna Murata 605, 00143 Roma, Italy

CLAUDIO FACCENNA

Dip. di Scienze della Terra, Università "La Sapienza", P.le Aldo Moro 5, 00185 Roma, Italy

RENATO FUNICIELLO

Istituto Nazionale di Geofisica, Via di Vigna Murata 605, 00143 Roma, Italy

and

MASSIMO MATTEI

Dip. di Scienze della Terra, III Università di Roma, Via C. Segre 2, 00154 Roma, Italy

(*Received* 9 *July* 1993; *accepted in revised form* 16 *November* 1993)

Abstract—Results are presented of structural analysis and anisotropy of magnetic susceptibility (AMS) analysis of Plio-Pleistocene clayey units from the extensional Tyrrhenian margin of central Italy. Data have been collected in different tectonic settings, mainly strike-slip and transverse extensional structures. At the sites with major evidence of Plio-Pleistocene tectonics, there appears a close relationship between magnetic lineations and stretching directions. Stretching processes that were able to modify the original magnetic fabric pre-dated significant normal-fault-related tilting, and therefore were active at the very first stage of extensional deformation. The relationships between AMS and structural trends in an extensional regime seem distinctively different from those reported in compressional regimes. This kind of analysis may be useful in the geodynamic interpretation of ambiguous structures.

INTRODUCTION

ANISOTROPY of magnetic susceptibility (AMS) analysis is an accurate, non-destructive and relatively fast technique of magnetic fabric determination and has been widely used for the study of strain pattern in deformed rocks. Relationships between magnetic fabric and structural setting were first described in sedimentary rocks of the Appalachians (Graham 1966). During the past 25 years, AMS analyses in relation to strain investigations have progressively increased (for a review see Hrouda 1982, Borradaile 1988, Lowrie 1989, Jackson & Tauxe 1991). Qualitative agreement between AMS and finite strain ellipsoids has been documented in several structural settings and rock types (see Kligfield *et al.* 1977, Turner & Gough 1983, Lowrie & Hirt 1987, Averbuch *et al.* 1992). AMS analysis of the strain pattern affecting weakly deformed, or apparently 'undeformed', clayey units in compressional regimes from Neogene orogenic belts has also been reported (Kissel *et al.* 1986, Lee *et al.* 1990, Sagnotti & Speranza 1993). In extensional regimes, these kinds of analyses have not yet been performed. Thus, no information exists, either on the possible relationship between a sedimentary magnetic fabric and extensional finite strain ellipsoid, or on the question of whether extensional tectonics overprints a tectonic fabric on the original fabric of a sediment.

This paper presents AMS results in an extensional tectonic regime, the central Italy Tyrrhenian margin, where a detailed structural analysis has been carried out, both at the regional and local scale. Within the context of the tectonic framework, the relationships between the magnetic fabric and the structural setting in weakly deformed sedimentary sequences will be discussed. The AMS and structural data have been collected in marine clayey deposits, filling basins developed from Messinian up to Lower Pleistocene.

GEOLOGICAL AND STRUCTURAL SETTING

The central Italy Tyrrhenian margin (Fig. 1) is characterized by a system of extensional basins, mostly oriented NW–SE to NNW–SSE, filled by clastic marine and continental deposits from Messinian up to Lower Pleistocene (Funiciello *et al.* 1981). During this time interval the extensional tectonics progressively migrated eastward, following the compressional phases related to the build-up of the Apennines (Elter *et al.* 1975, Patacca *et al.* 1990). At the same time in the Tyrrhenian margin

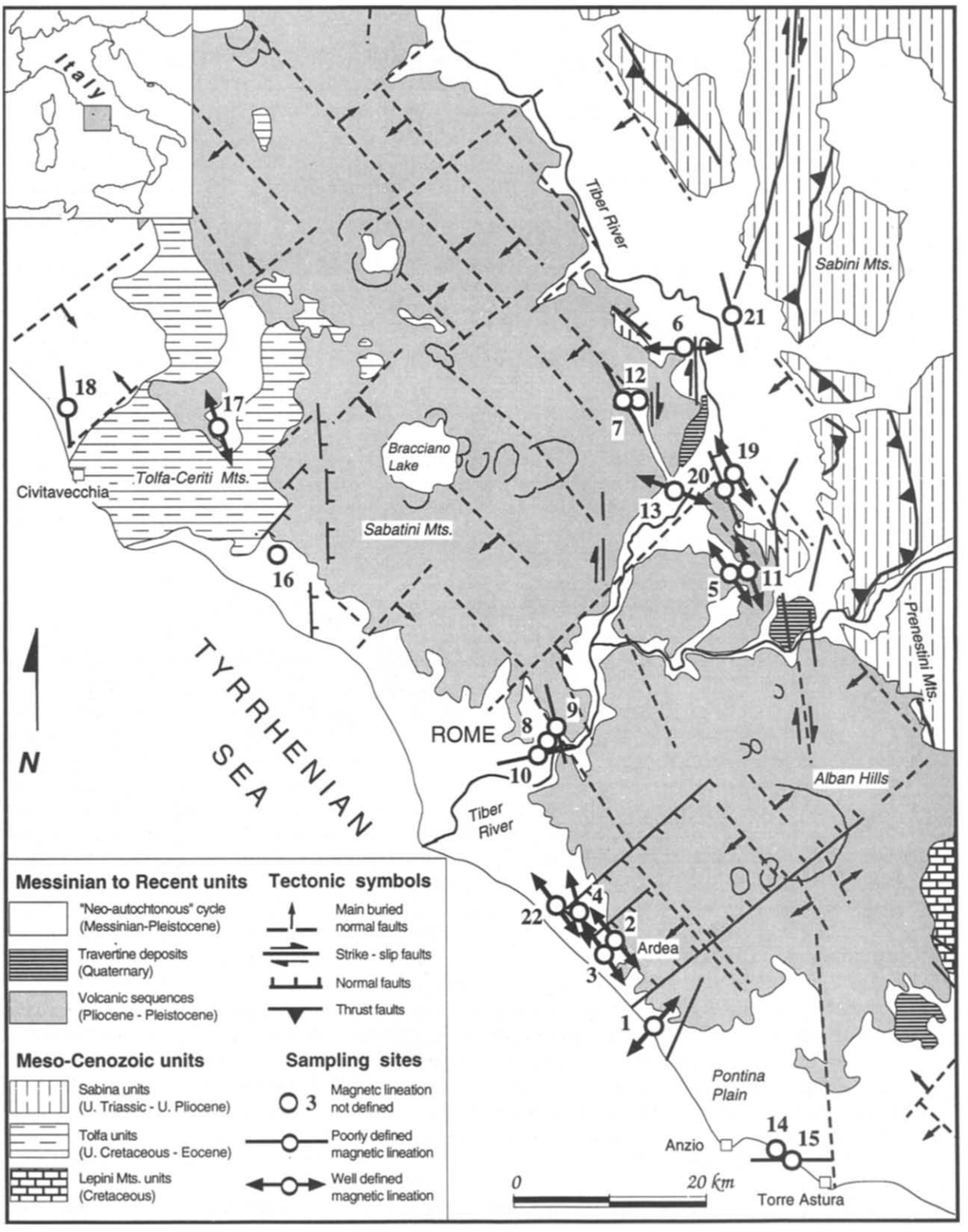

Fig. 1. Geological sketch map of the central Italy Tyrrhenian margin and location of the sampling sites.

minor NE–SW-oriented basins developed, as transfer-related features. They are filled with up to 2500 m of syn-rift and post-rift sediments and are bounded by purely dip-slip normal faults that define an overall half-graben geometry (Mariani & Prato 1988).

In the area studied, right-lateral strike-slip faults were active during middle–upper Pleistocene (Funiciello *et al.* 1992, Faccenna *et al.* in press). These faults, with a N–S bearing, define narrow N–S shear zones formed by few kilometers long discrete segments in a dextral en échelon array. Two main strike-slip fault zones, 30–40 km long and less than 20 km wide, between the Sabini mountains and the Alban Hills volcanic district, have been distinguished.

Magmatic activity accompanied and followed crustal extension in the Tyrrhenian margin of Central Italy, with the development of large volcanic complexes (Locardi *et al.* 1977). In the study area magmatic activity started during the Pliocene in the Tolfa–Ceriti area and reached a climax during the Middle–Upper Pleistocene, with the high-potassium volcanism of the Roman Co-magmatic Province.

The overall deformation is mainly represented by normal and strike-slip faults and extensional joint systems (no cleavage or ductile elements are recognizable in the field), with a peculiar superficial brittle deformation style. The extension is exhibited by the development of half-grabens and related passive structures (roll-overs and antiform flexures due to hanging-wall uplift) and vertical uplift of structural blocks.

SAMPLING AND MEASUREMENTS

Samples were collected at 22 sites (215 oriented cores) in Messinian–Lower Pleistocene clayey units from the central Italy Tyrrhenian margin, between Civitavecchia and Torre Astura (Fig. 1). Blue–grey colours in the fine-grained sediments were preferred to avoid possible weathering effects. Sampling was performed by *in situ* drilling with a portable gasoline engine, driving a 25 mm corer with a water-cooled diamond impregnated cutting head. In this area the Messinian–Pleistocene marine clayey units are often overlain by volcanic and continental deposits. Thus, the availability of suitable outcrops influenced the sampling site distribution. First, a homogeneous coverage was made of the whole area. Then an increase in sampling density was made at those places of major interest. The sampled units are generally sub-horizontal and weakly deformed, with sets of joints and faults, or even apparently undeformed. At each site the orientation of the mesoscopic fabric elements (bedding, joints, faults) was measured and a structural analysis was performed. The orientation of the stress tensor axis has been reconstructed with the program of Angelier & Gouguel (1979) by using fault planes and related striations. Extensional joints are often filled with calcite and gypsum mineralizations, related to hydrothermal circulation (Maiorani *et al.* 1992). The poles of these joint planes have been used to determine the local direction of stretching.

Nine sites are located in the Tiber valley north of Rome, where sub-horizontal Plio-Pleistocene clayey deposits are affected by N–S right-lateral strike-slip faults. Three sites were sampled in Rome, in sub-horizontal Plio-Pleistocene marine deposits. Five sites are in the Ardea extensional basin, NE–SW-oriented, in tilted Plio-Pleistocene sequences. Two other sites were sampled along the coast just south of Anzio (Torre Astura). Three more sites are in clayey units from the Messinian–Pliocene extensional basins of the Tolfa–Ceriti Mountains.

From each oriented core, one to four cylindrical specimens (25 mm diameter × 22 mm height) were sliced and a specimen for each core was measured with a KLY-2 Kappabridge (Geofyzika Brno) in the paleomagnetic laboratory of the Istituto Nazionale di Geofisica. The susceptibility tensor for each specimen was computed by the ANISO 11 program (Jelinek 1977) and the site data were grouped and evaluated statistically using the ANS 21 program (Jelinek 1978). For the representation of the specimens and sites magnetic fabric the F, L, P' and T anisotropy parameters were computed (Table 1).

RESULTS

The mean susceptibility of the specimens is fairly low; the mean value for each site ranges between 7.2×10^{-5} (LZ21) and 3.4×10^{-4} (LZ14) SI units, with generally limited standard deviations. Though detailed mineralogical analyses should be necessary for a proper definition of the mineral carriers of the measured susceptibility, the observed range of values suggests roughly that the contributions of the ferromagnetic fraction cannot be relevant (see Hrouda & Kahan 1991). Otherwise, hysteresis loops performed on clayey units from the Central Apennines with similar susceptibility values (Averbuch 1993) demonstrate that the main contribution to the susceptibility is given by the phyllosilicate paramagnetic matrix.

The observed magnetic fabrics are typical of undeformed or at least weakly deformed sediments. The anisotropy degree is low, with values of P' generally well below 1.1 (Fig. 2). Ellipsoid shapes for each site vary from rotational oblate to triaxial, with the k_{min} axes always clustered around the bedding poles (Fig. 3). Some sites show the k_{max} and the k_{int} axes scattered in the bedding plane (rotational oblate susceptibility ellipsoid). At many sites a clearly distinct magnetic lineation is defined by the clustering of the k_{max} axes. A magnetic lineation has been considered well defined when the semi-angle of the 95% confidence ellipse in the $k_{max} - k_{int}$ plane (the e_{12} angle) is <30°, poorly defined when $30° \leq e_{12} \leq 45°$ and not defined at all when $e_{12} > 45°$ (Fig. 1 and Table 1).

AMS data (anisotropy degree, ellipsoid shapes and orientations) are quite constant for each tectonic struc-

Table 1. List of anisotropy factors computed at each site

Sites	N	k_m	L	F	P'	T	e_{12}
LZ05	13	106.9 (4.3)	1.010(0.002)	1.017 (0.006)	1.027(0.005)	0.203(0.253)	
			1.009	1.016	1.026	0.278	10.1
LZ11	10	105.6 (3.0)	1.006(0.003)	1.023(0.006)	1.031(0.006)	0.542(0.198)	
			1.006	1.021	1.029	0.533	13.7
LZ19	16	148.0(57.0)	1.004(0.002)	1.027(0.008)	1.035(0.009)	0.717(0.210)	
			1.004	1.027	1.033	0.741	8.1
LZ20	8	117.0 (8.6)	1.004(0.002)	1.031(0.006)	1.039(0.006)	0.746(0.133)	
			1.003	1.031	1.038	0.819	34.0
LZ06	8	83.3 (8.5)	1.004(0.003)	1.024(0.014)	1.031(0.017)	0.742(0.130)	
			1.003	1.024	1.030	0.748	17.1
LZ13	9	145.8(6.4)	1.012(0.007)	1.013(0.011)	1.027(0.009)	−0.054(0.563)	
			1.010	1.013	1.024	0.110	15.1
LZ21	8	72.0 (6.6)	1.003(0.001)	1.020(0.004)	1.025(0.004)	0.703(0.079)	
			1.002	1.020	1.025	0.831	41.8
LZ07	12	102.5 (5.0)	1.004(0.003)	1.029(0.007)	1.037(0.007)	0.723(0.211)	
			1.003	1.029	1.035	0.835	31.8
LZ12	9	104.3 (3.2)	1.004(0.003)	1.022(0.004)	1.029(0.004)	0.723(0.225)	
			1.000	1.023	1.027	0.973	82.9
LZ08	9	127.8 (5.0)	1.003(0.002)	1.050(0.004)	1.059(0.004)	0.882(0.094)	
			1.001	1.050	1.059	0.957	60.6
LZ09	10	117.9 (9.1)	1.002(0.001)	1.032(0.010)	1.038(0.012)	0.868(0.045)	
			1.002	1.029	1.035	0.896	38.9
LZ10	10	155.6 (9.5)	1.003(0.001)	1.036(0.005)	1.043(0.006)	0.822(0.058)	
			1.002	1.036	1.043	0.889	30.3
LZ02	8	158.1(41.6)	1.004(0.002)	1.024(0.005)	1.031(0.006)	0.712(0.111)	
			1.003	1.024	1.030	0.747	20.9
LZ03	8	79.5 (2.1)	1.007(0.003)	1.016(0.004)	1.024(0.003)	0.414(0.284)	
			1.006	1.016	1.023	0.416	12.8
LZ04	7	131.7 (8.9)	1.001(0.001)	1.009(0.003)	1.011(0.004)	0.718(0.167)	
			1.001	1.009	1.011	0.756	19.1
LZ22	10	105.2 (5.5)	1.003(0.001)	1.012(0.001)	1.017(0.002)	0.566(0.133)	
			1.003	1.012	1.016	0.584	13.3
LZ01	11	83.4(13.8)	1.005(0.002)	1.016(0.002)	1.022(0.002)	0.527(0.174)	
			1.004	1.016	1.021	0.547	12.3
LZ14	10	339.1(27.5)	1.007(0.005)	1.017(0.009)	1.026(0.008)	0.340(0.503)	
			1.002	1.016	1.020	0.750	53.8
LZ15	10	297.6(75.8)	1.005(0.002)	1.021(0.004)	1.027(0.004)	0.614(0.185)	
			1.003	1.020	1.025	0.739	31.6
LZ17	9	157.0(11.4)	1.008(0.001)	1.078(0.011)	1.096(0.013)	0.798(0.037)	
			1.008	1.076	1.094	0.795	5.7
LZ18	10	171.5(10.1)	1.003(0.001)	1.026(0.006)	1.032(0.007)	0.803(0.074)	
			1.002	1.026	1.031	0.885	32.3

The upper line for each locality shows the arithmetic means of the individual specimen values (standard deviation in parentheses); the lower line shows the locality tensorial means. Site LZ16 was disregarded (see text).

N=number of samples.

$k_m = (k_{max} + k_{int} + k_{min})/3$ (mean susceptibility, in 10^{-6} SI units).

$L = k_{max}/k_{int}$ (lineation).

$F = k_{int}/k_{min}$ (foliation).

$P' = \exp\sqrt{2[(\eta_1 - \eta)^2 + (\eta_2 - \eta)^2 + (\eta_3 - \eta)^2]}$ (corrected anisotropy degree).

$T = 2(\eta_2 - \eta_3)/(\eta_1 - \eta_3) - 1$ (shape factor).

$\eta_1 = \ln k_{max}$, $\eta_2 = \ln k_{int}$, $\eta_3 = \ln k_{min}$, $\eta = (\eta_1 + \eta_2 + \eta_3)/3$.

e_{12}: semi-angle of the 95% confidence ellipse around the mean k_{max} axis in the $k_{max} - k_{int}$ plane.

ture. Data from each site have been grouped according to their location with respect to the local and regional structural setting. Each group will now be examined in detail.

Tiber valley north of Rome

Guidonia, UNICEM quarry. Two sites (LZ05 and LZ11) were sampled at two different quarry faces, in sub-horizontal Pliocene clays, affected by extensional joints and strike-slip faults, whose calcite fillings have been dated at 50,000 and 178,000 y, respectively (Funiciello *et al.* 1992). AMS data are quite similar at the two sites giving a mean triaxial susceptibility ellipsoid with each of the principal axes well defined and tightly grouped. The k_{max} axes, in the horizontal plane, strictly reflects the maximum extensional axis direction (Fig. 4).

Vallericca, Tini quarry. Two sites (LZ19 and LZ20) were sampled at the bottom and the top of the outcropping sequence, respectively, in sub-horizontal upper Pliocene clayey units. The magnetic fabric and the structural setting are quite similar to the ones observed at the UNICEM quarry (Fig. 5).

Tiber west bank. Two sites (LZ06 and LZ13), about 15

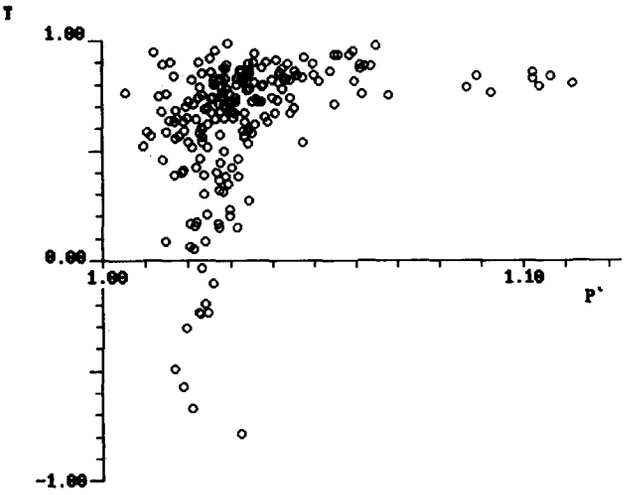

Fig. 2. Magnetic anisotropy plot of the analysed specimens. P' indicates the anisotropy degree (computed by all the three principal susceptibilities), T the shape of the susceptibility ellipsoid ($T = +1$: planar magnetic fabric and uniaxial oblate ellipsoid; $T = -1$: linear magnetic fabric and uniaxial prolate ellipsoid; $T > 0$: oblate ellipsoid; $T < 0$ prolate ellipsoid; $T = 0$: neutral or triaxial ellipsoid). Specimens with $P' > 1.08$ are from site LZ17. Specimens with $T < 0$ are from sites LZ05, LZ13 and LZ19.

km apart, were sampled in Pleistocene units, along the west bank of the Tiber river. The LZ06 samples were taken from two clayey levels in a sub-horizontal coarse grained sequence. The LZ13 samples were taken in a slump within a sub-horizontal sandy–clayey sequence. AMS data are quite defined at both sites, with triaxial susceptibility ellipsoids and k_{max} axes clustered around N108° (Fig. 6), indicating that the magnetic fabric at site LZ13 was acquired after the slumping perturbation. In the area between the two sites the structural analysis points out a NNE–SSW Plio-Pleistocene maximum compressional axis.

Further north in the Tiber valley one more site (LZ21) was sampled in a sub-horizontal lower Pleistocene sandy–clayey unit. AMS data indicate a mean oblate ellipsoid, with the horizontal k_{max} axes weakly grouped NNW–SSE.

San Martino valley. Two sites (LZ07 and LZ12) were sampled in tilted Upper Pliocene–Lower Pleistocene clays, with opposite bedding dip. AMS ellipsoids are strongly oblate. The combined AMS data from the two sites define a faint magnetic lineation, which is better defined, trending N327°, after tectonic correction (the e_{12} angle reduces from 54.2 to 36.6). No tectonic element affects the clays at the sampling sites; however, along the stream valley a system of discontinuous Pleistocene strike-slip faults and a NNW–SSE maximum extensional axis were recognized (Fig. 7).

In summary, the total Tiber valley AMS data show an anisotropy degree always below 1.06 and ellipsoid shapes predominantly oblate. Only a few specimens exhibit prolate ellipsoids. The ellipsoid orientation is constant (Fig. 8), with the k_{min} clustered vertical and the k_{max} defining a general magnetic lineation trend of N322°.

Rome

Three sites (LZ08, LZ09 and LZ10) were sampled from the centre of Rome, in a Plio-Pleistocene sub-horizontal marly–clayey sequence exposed at Monte Mario. No evident tectonic feature is present at the sampling sites. AMS data are similar at the three sites: susceptibility ellipsoids are strongly oblate with very weak magnetic lineations. The overall analysis displays a typical sedimentary fabric, with a rotational oblate susceptibility ellipsoid (Fig. 9).

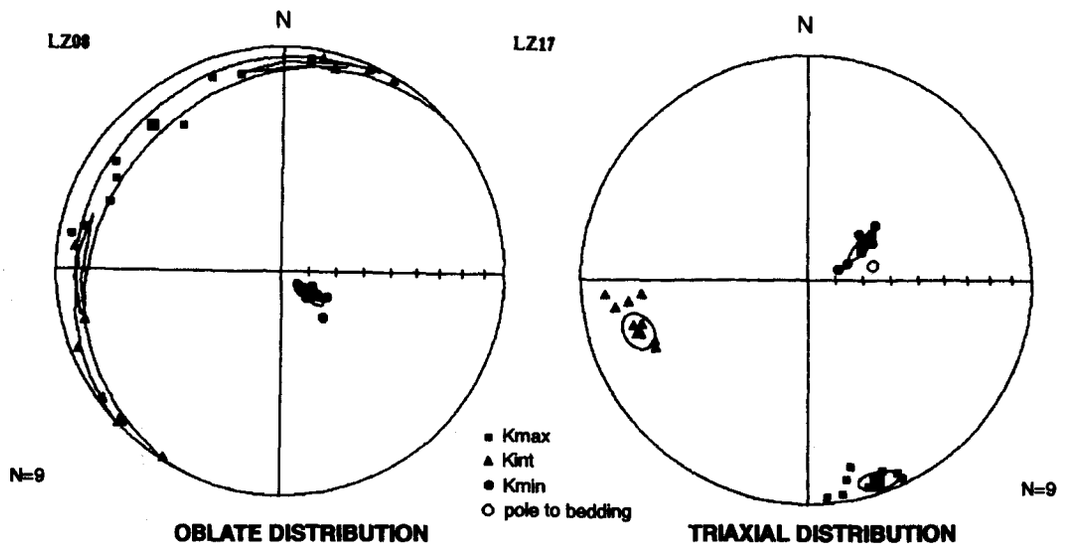

Fig. 3. Magnetic fabrics at sites LZ08 and LZ17. Schmidt equal-area projections, lower-hemisphere. Around each of the mean principal susceptibility axes, the related 95% confidence ellipses are drawn. LZ08: magnetic ellipsoid strongly oblate; the k_{min} axes are tightly clustered on the bedding pole, the other two axes are scattered in the bedding plane. LZ17: triaxial magnetic ellipsoid; each of the k axes is tightly grouped.

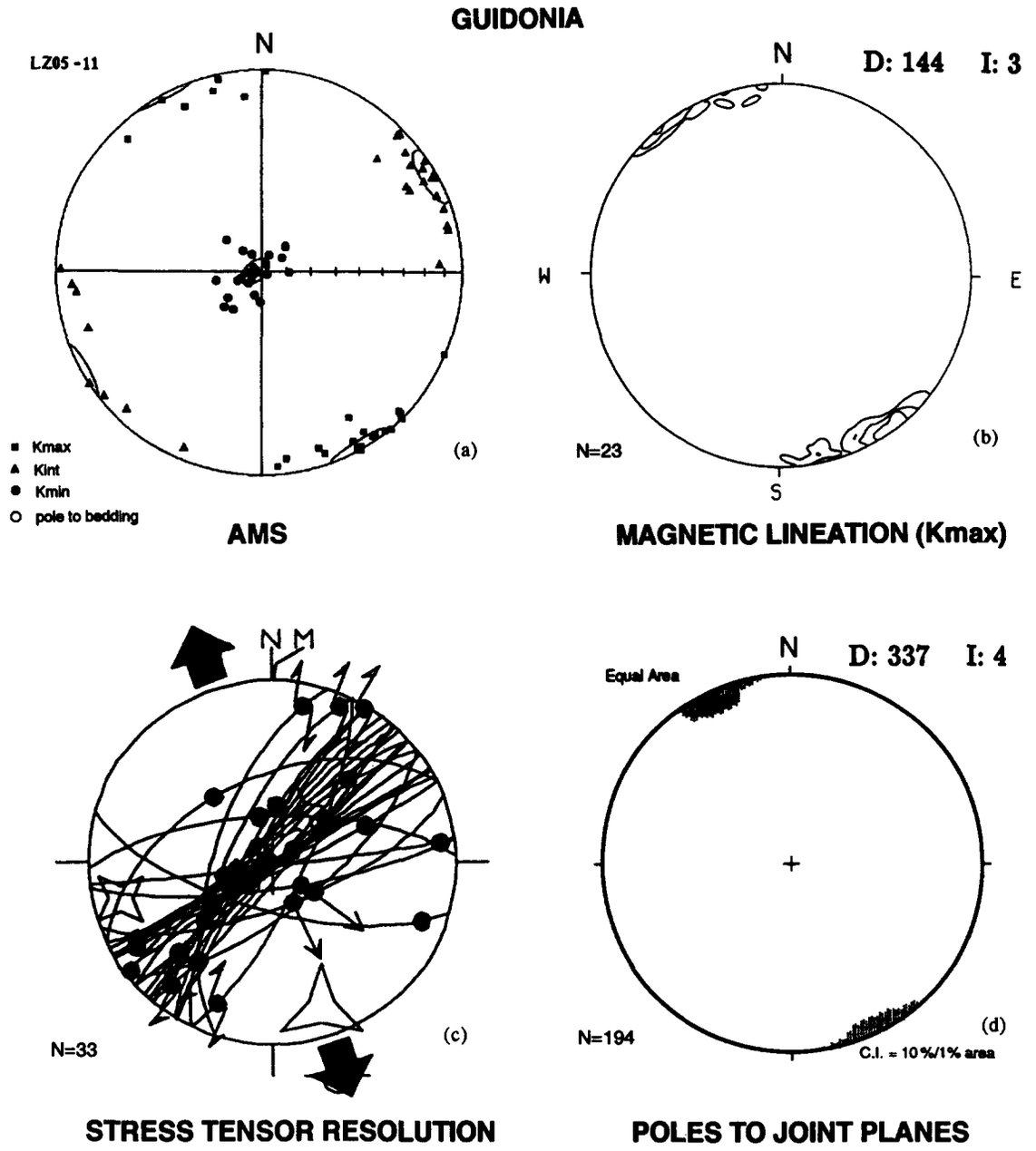

Fig. 4. Magnetic fabric and structural measurements at sites LZ05 and LZ11 (Guidonia). Schmidt equal-area projections, lower-hemisphere. (b) & (d) The contour interval is 10%, the maximum density direction (D = declination; I = inclination) is reported at the top right. (c) Points and arrows on the fault traces correspond to the measured striations, large black arrows indicate the computed minimum stress direction. Big open stars indicate the computed principal stress axes.

Ardea basin

Four sites (LZ02, LZ03, LZ04 and LZ22) were sampled in Upper Pliocene–Lower Pleistocene clayey units filling the Ardea extensional basin. This half-graben basin, 10 km wide and more than 2000 m deep, is characterized by a set of NE–SW-oriented normal faults. Typical roll-over geometries are present in proximity of the main faults, with the hanging wall tilted up to 30°. During the Upper Pliocene, coeval to the basin growth, a fast footwall uplift occurred in the Anzio area with the formation of a broad anticline flexure, parallel to the basin axis. Sites LZ02, LZ03 and LZ04 are inside the half-graben, in opposite dipping tilted blocks. Sites LZ04 and LZ22 are on the hanging-wall and foot-wall of the main antithetic fault, respectively.

AMS data indicate mean triaxial ellipsoids with the k_{int} and k_{max} axes well defined in the bedding plane (Fig. 10). At the three sites inside the half-graben the magnetic lineations are parallel to the bedding dips, with an orientation of NW–SE. Also, at site LZ22 the magnetic lineation is sub-parallel to the other three sites. The overall analysis of sites in and around the graben shows that the tectonic correction for the dip of the strata results in a better grouping of each of the k clusters (Fig. 11). The magnetic lineation is sub-horizontal and trends N320°, parallel to the poles of the extensional joints and orthogonal to the basin axis.

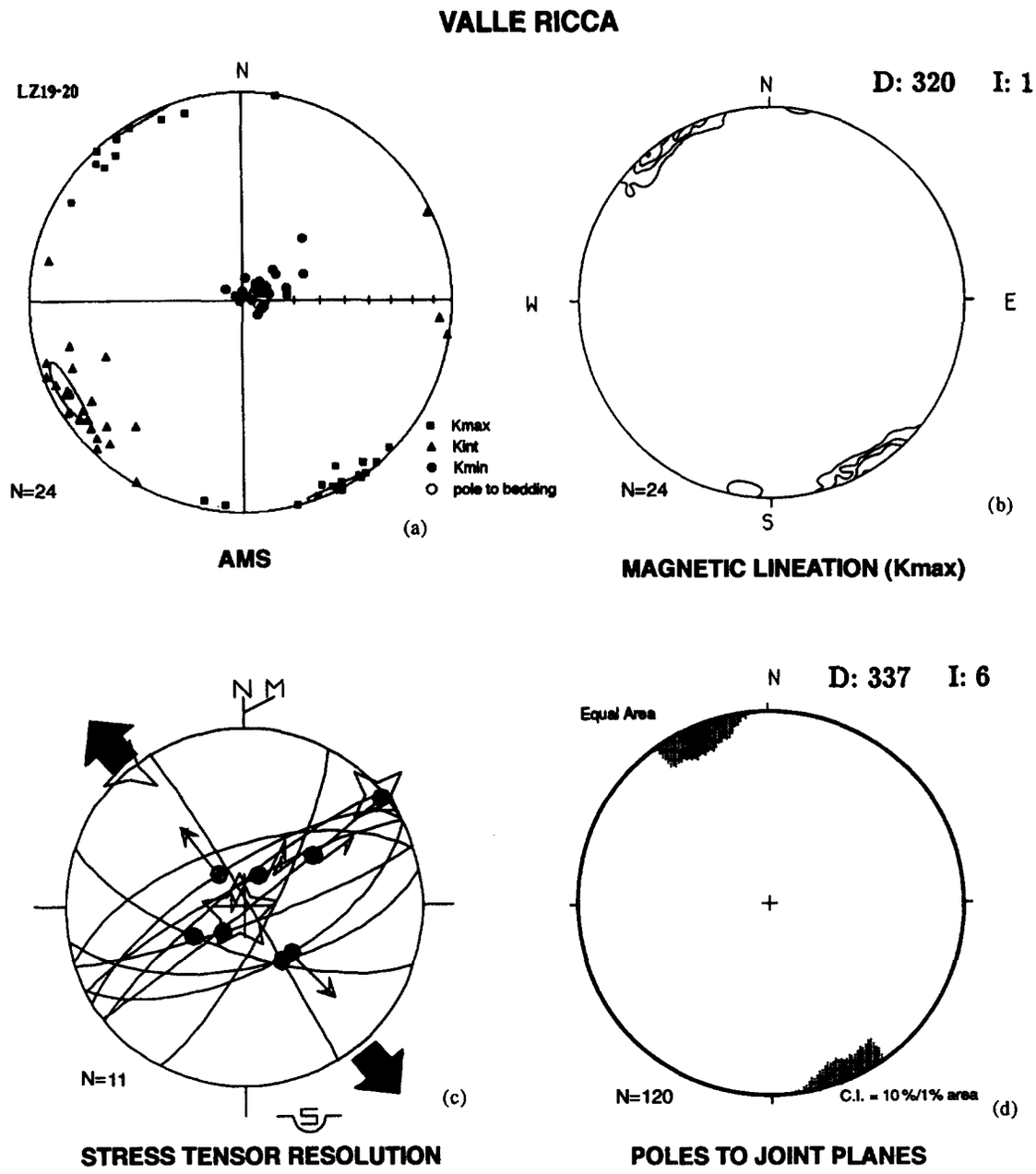

Fig. 5. Magnetic fabric and structural measurements at sites LZ19 and LZ20 (Valle Ricca). Schmidt equal-area projections, lower-hemisphere. (b) & (d) The contour interval is 10%, the maximum density direction (D = declination; I = inclination) is reported at the top right. (c) Points and arrows on the fault traces correspond to the measured striations, large black arrows indicate the computed minimum stress direction. Big open stars indicate the computed principal stress axes.

One site (LZ01) was sampled in the Pliocene clays along the shoreline north of Anzio, on the eastern flank of the anticline flexure. AMS data show a mean triaxial ellipsoid with the k_{max} grouped horizontally along the axis of the flexure, trending around N30° (Fig. 10).

Torre Astura

Two sites (LZ14 and LZ15) were sampled in a Pliocene clayey unit along the shoreline south of Anzio. Neither bedding nor structural elements are evident at these sites. AMS data yield mean susceptibility ellipsoids with none of the principal susceptibilities tightly clustered. The k_{min} are more or less vertical, the other two axes are scattered in the horizontal plane (Fig. 12).

Tolfa–Ceriti Mountains

Three sites (LZ16, LZ17 and LZ18) were sampled around Upper Pliocene acidic lava domes. LZ16 and LZ17 are in Messinian clays with bands and lenses of microcrystalline gypsum. In particular, a pervasive lamination makes the sedimentary fabric evident at site LZ17. AMS data from site LZ16 are difficult to interpret and probably arise from two interfering anisotropic sources: some samples are very weakly anisotropic, with

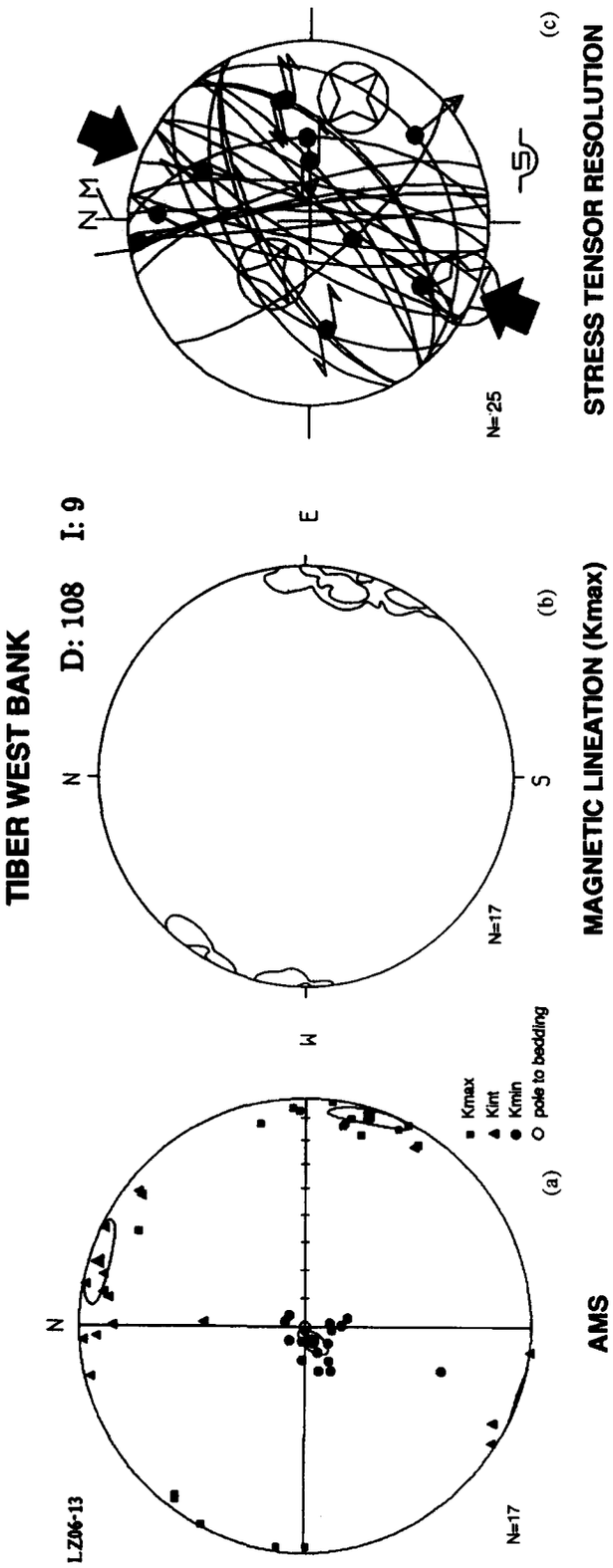

Fig. 6. Magnetic fabric and structural measurements (only fault planes are shown) at sites LZ06 and LZ13 (Tiber west bank). Schmidt equal-area projections, lower-hemisphere (b) The contour interval is 10%, the maximum density direction (D = declination; I = inclination) is reported at the top right. (c) Points and arrows on the fault traces correspond to the measured striations, large black arrows indicate the computed maximum stress direction. Big open stars indicate the computed principal stress axes.

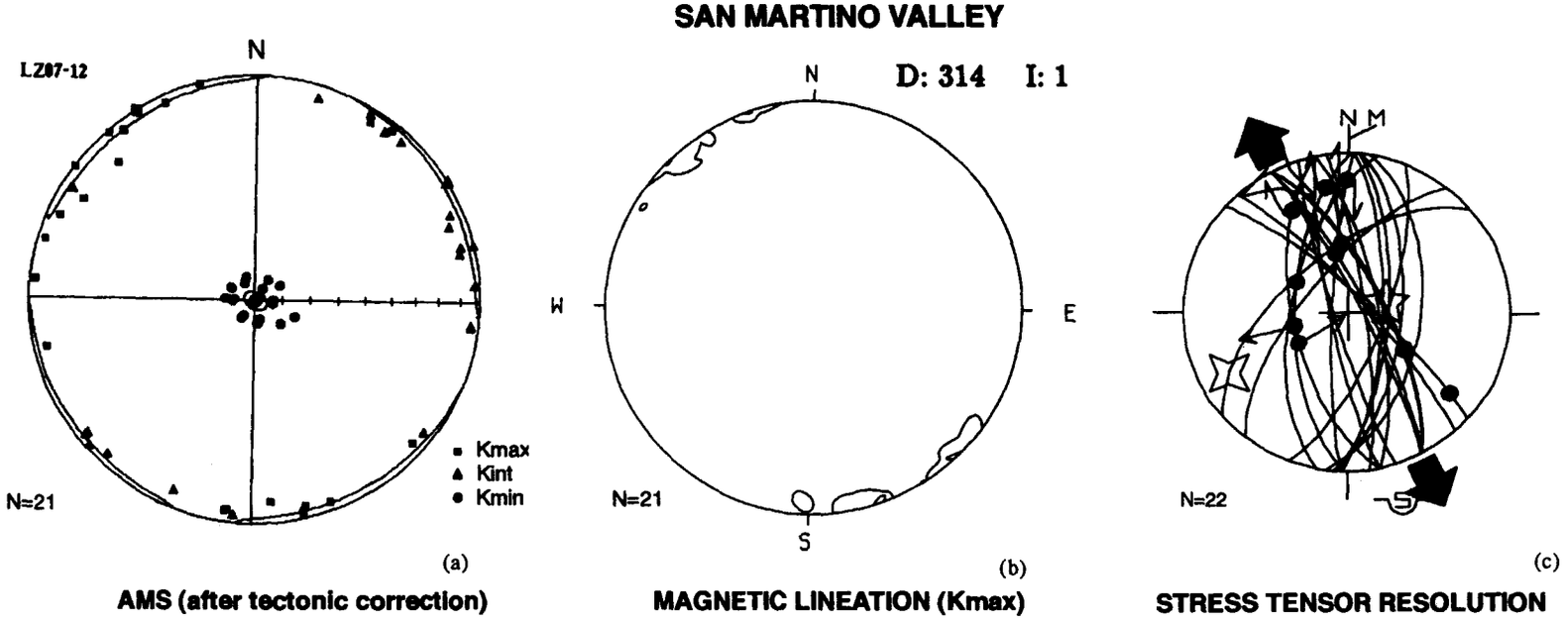

Fig. 7. Magnetic fabric and structural measurements (only fault planes are shown) at sites LZ07 and LZ12 (San Martino Valley). Schmidt equal-area projections, lower-hemisphere. (b) The contour interval is 10%, the maximum density direction (D = declination; I = inclination) is reported at the top right. (c) Points and arrows on the fault traces correspond to the measured striations, large black arrows indicate the computed minimum stress direction. Big open stars indicate the computed principal stress axes.

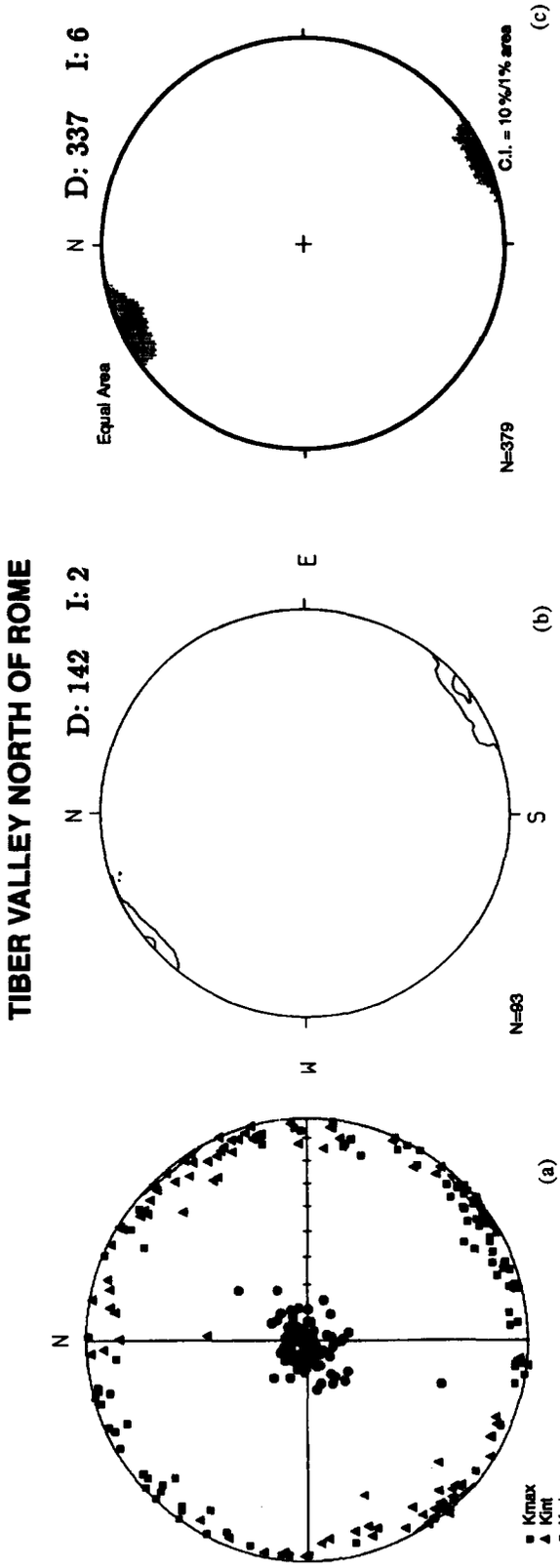

Fig. 8. Total AMS (after tectonic correction) and joints planes plots for the Tiber valley north of Rome. Schmidt equal-area projections, lower-hemisphere. (b) & (c) The contour interval is 10%, the maximum density direction (D = declination; I = inclination) is reported at the top right.

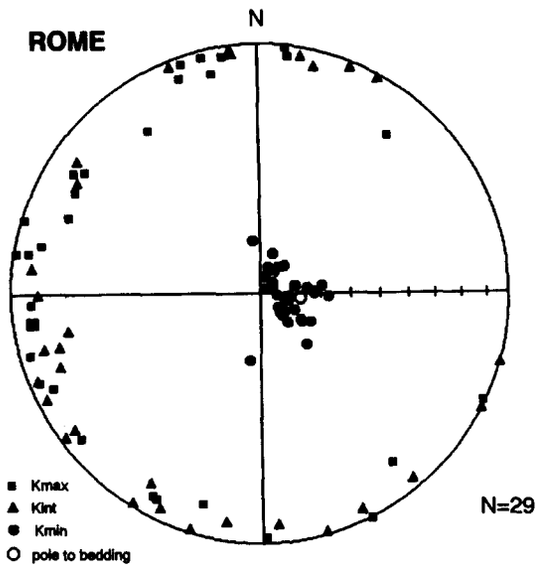

Fig. 9. Orientation of the magnetic anisotropy ellipsoid axes for the specimens from the three sites in Rome (LZ08, LZ09 and LZ10). Schmidt equal-area projection, lower-hemisphere.

k_{min} vertical and oblate ellipsoids; other samples are more anisotropic, with k_{max} vertical and prolate ellipsoids. AMS results from LZ17 are more consistent. They yield the highest anisotropy degree found in this study ($P' = 1.094$) and the highest degree of magnetic foliation ($F = 1.076$). Also, a distinct NNW–SSE magnetic lineation is present (Fig. 3). LZ18 is in Pliocene blue–grey clays. A set of normal faults was recognized at the sampling site, indicating NNW–SSE extension (Fig. 13). The mean susceptibility ellipsoid is strongly oblate, with a weak magnetic lineation, parallel to the maximum extensional axis.

DISCUSSION

At all the sites, the magnetic fabrics are typical of undeformed or weakly deformed sediments. The k_{min} axes are grouped around the bedding poles and the mean susceptibility ellipsoids are predominantly oblate. Moreover, many sites are characterized by a well-defined magnetic lineation in the bedding plane. The direction of these magnetic lineations strictly agrees with the local stretching axis, calculated from structural analysis. In particular, there is a close agreement between the k_{max} clusters, the grouping of extensional joint poles and the maximum extensional axis reconstructed by fault slip vectors analysis. This agreement is confirmed at a local scale. For example, at sites LZ05 and LZ11 in the UNICEM quarry, AMS and structural data both show a small difference (15°) between the two sites (Fig. 14).

The gradual development of a magnetic lineation can provide a preliminary evaluation of the relative degree of strain between different sites. Therefore, qualitative to semiquantitative relationships between AMS data and strain, well documented in many compressional regimes, appear to be valid in this study of weakly deformed clayey units in an extensional, locally strike-slip, tectonic regime. However, the relationships between AMS and the bedding attitude in an extensional regime seem to be different from those typical of the compressional ones. In the first stages of compressional deformation the magnetic lineation follows the structural trends (fold axes and thrusts). In the extensional basins analysed here, the magnetic fabric shows a lineation orthogonal to the general trend of the tectonic structures; i.e. parallel to the bedding dips in roll-over antiform with rotational normal faults (Ardea basin). In

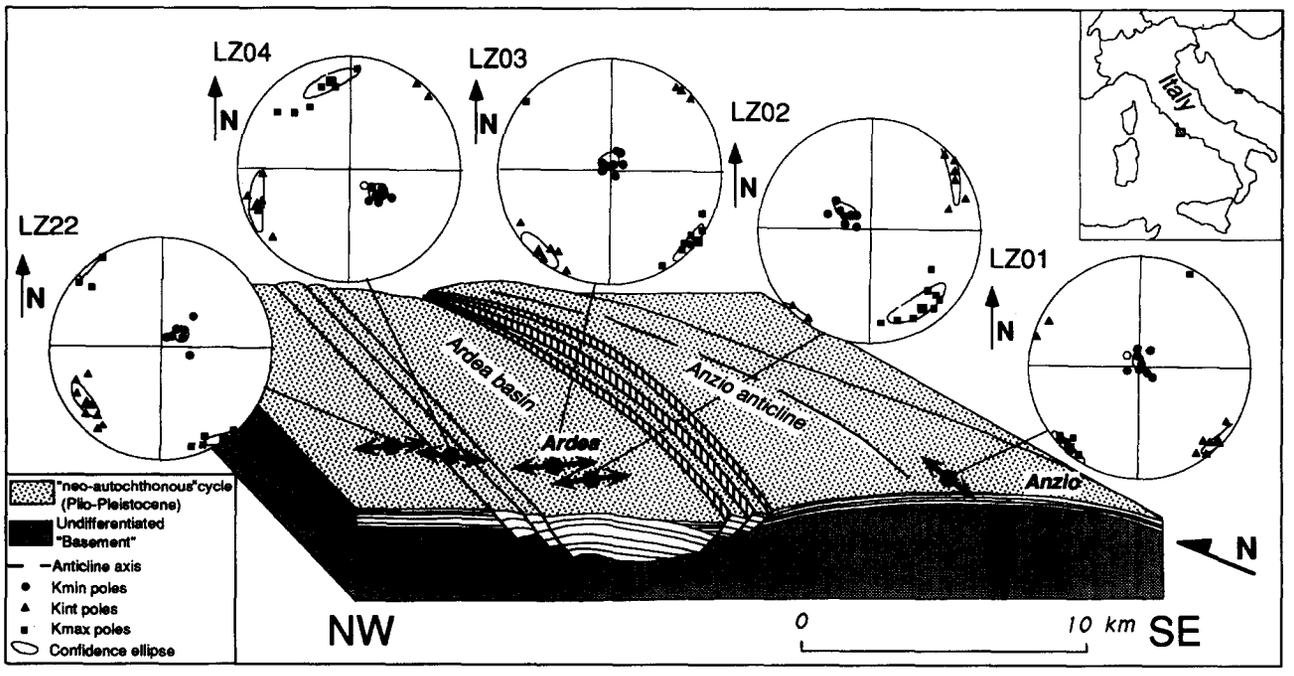

Fig. 10. Schematic block-diagram of the Ardea basin and AMS plots for the LZ01–02–03–04–22 sites.

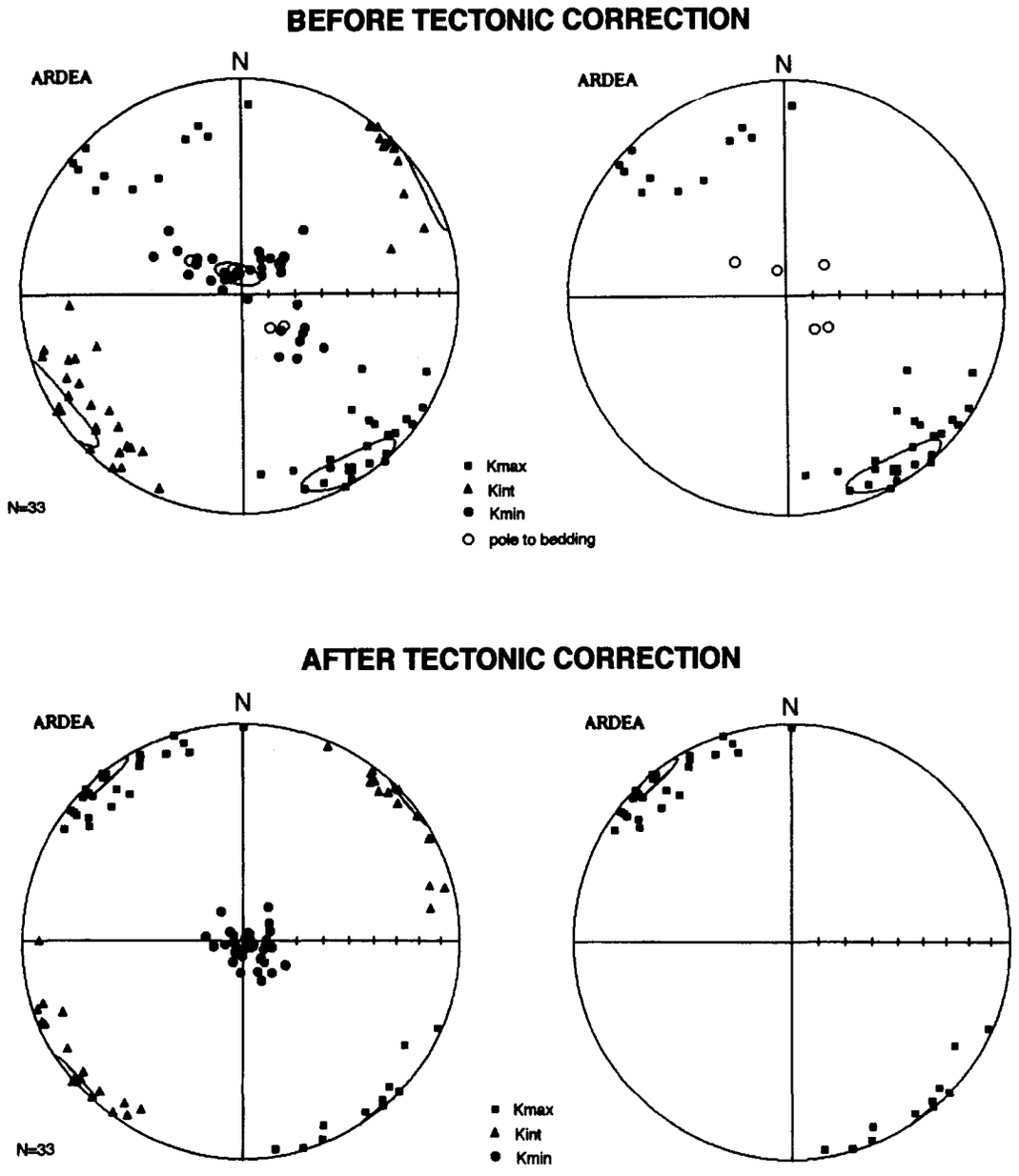

Fig. 11. Magnetic fabrics and magnetic lineations at four sites (LZ02, LZ03, LZ04 and LZ22) in the Ardea basin, before and after tectonic correction. Schmidt equal-area projections, lower hemisphere. After tectonic correction the semi-angles of the 95% confidence ellipses around the mean directions are about half of the value before tectonic correction (the e_{12} angle decreases from 14.8 to 8.0).

the studied area parallelism between magnetic lineation and structural trend has been observed only in the Anzio flexure. In this case the magnetic lineation is orthogonal to the basin extensional axis; however it is parallel to the axis of the flexure linked to the isostatic footwall uplift. Hence, it seems to be controlled by the local shortening direction, oriented NW–SE.

In the strike-slip zones, where the Plio-Pleistocene sediments are sub-horizontal, parallelism between the magnetic lineation and the extensional axis is strongly confirmed.

In the Ardea basin, where it has been possible to apply a tectonic correction at each site, restoring bedding to paleo-horizontal, the AMS data indicate that the magnetic fabric was acquired before tilting. This implies that the stretching processes that caused partial reorientation of the original magnetic fabric were active at the earliest stage of the deformational history. In fact, the acquisition of a magnetic lineation parallel to the maximum stretching direction predates the normal faulting that caused the tilt of bedding; in other words, the observed AMS–strain relationships originated at the beginning of the basin growth. The process seems to work as follow: (1) the extension causes stretching in the clays that (overprinting a tectonic fabric on the sedimentary fabric) results in a well defined magnetic lineation in the bedding plane, parallel to the maximum stretching in that place; (2) movements on rotational normal faults tilt the bedding and originate roll-over structures; at this point the magnetic fabric is not further affected by

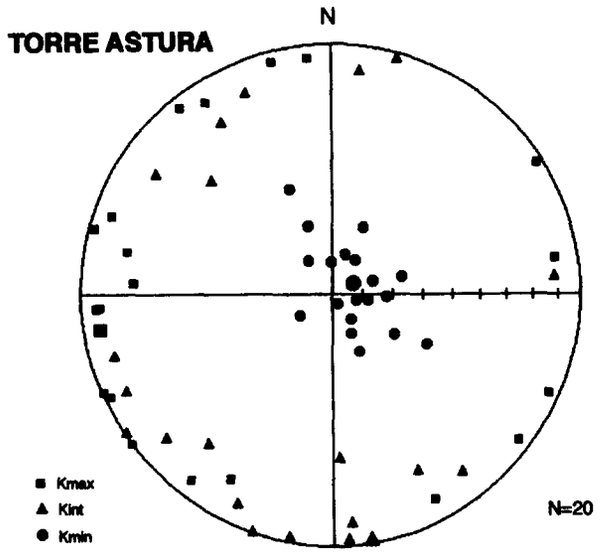

Fig. 12. Orientation of the magnetic anisotropy ellipsoid axes for specimens from two sites at Torre Astura (LZ14 and LZ15). Schmidt equal-area projection, lower-hemisphere.

tectonics and it is passively tilted together with strata. This process can be validated by the observation that the magnetic lineations follow the bedding dips at each site and group in a single cluster after the restoration of the bedding to the horizontal.

Due to the distinctive character of AMS–structural setting relationship in compressional and extensional settings, this kind of analysis seems particularly suitable in the study of propagating thrust belts, where small sedimentary basins can arise either by piggy-back mechanisms or by extensional processes related to orogenic collapse. A magnetic lineation should be parallel to the basin axis in the first case, and perpendicular to the basin axis in the other case.

The lack of magnetic lineation at the three sites in Rome (LZ08–10) indicates that the processes that produced the Monte Mario uplift did not affect the primary sedimentary magnetic fabric of the clayey units. In fact, the Pleistocene uplift of the Monte Mario ridge seems to be due to purely vertical movements. Therefore, in extensional regimes the acquisition of a tectonic magnetic lineation seems to be limited to the cases in which stretching processes play a major role.

The AMS and the structural data define a NW–SE extensional direction that is quite constant for wide areas. This strain pattern can be considered representative of a large-scale tectonic setting. However, this extensional trend is roughly orthogonal to the regional extensional direction (NE–SW) that characterized the Tyrrhenian margin since late Tortonian. In fact, we analysed transverse structures along which the NE–SW extension had no more than a subordinate significance. In these cases, the data indicate that the NW–SE extension, active along these structures during the Plio-Pleistocene, played a significant role in the overall geodynamic evolution of the central Italy Tyrrhenian margin and allowed the development of important tectonic structures and sedimentary basins.

CONCLUSIONS

Anisotropy of magnetic susceptibility data revealed essentially three different types of magnetic fabric which can be related to three different processes.

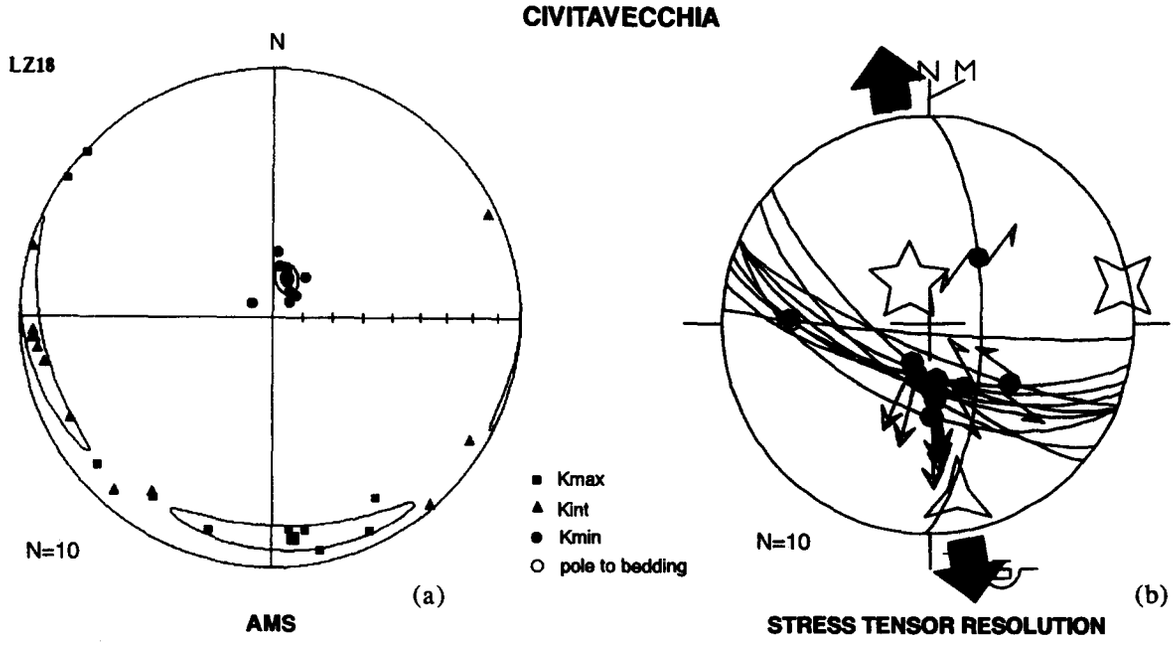

Fig. 13. Magnetic fabric and structural measurements (only fault planes are shown) at site LZ18 (Civitavecchia). Schmidt equal-area projections, lower-hemisphere. In (b), points and arrows on the fault traces correspond to the measured striations, large black arrows indicate the computed minimum stress direction. Big open stars indicate the computed principal stress axes.

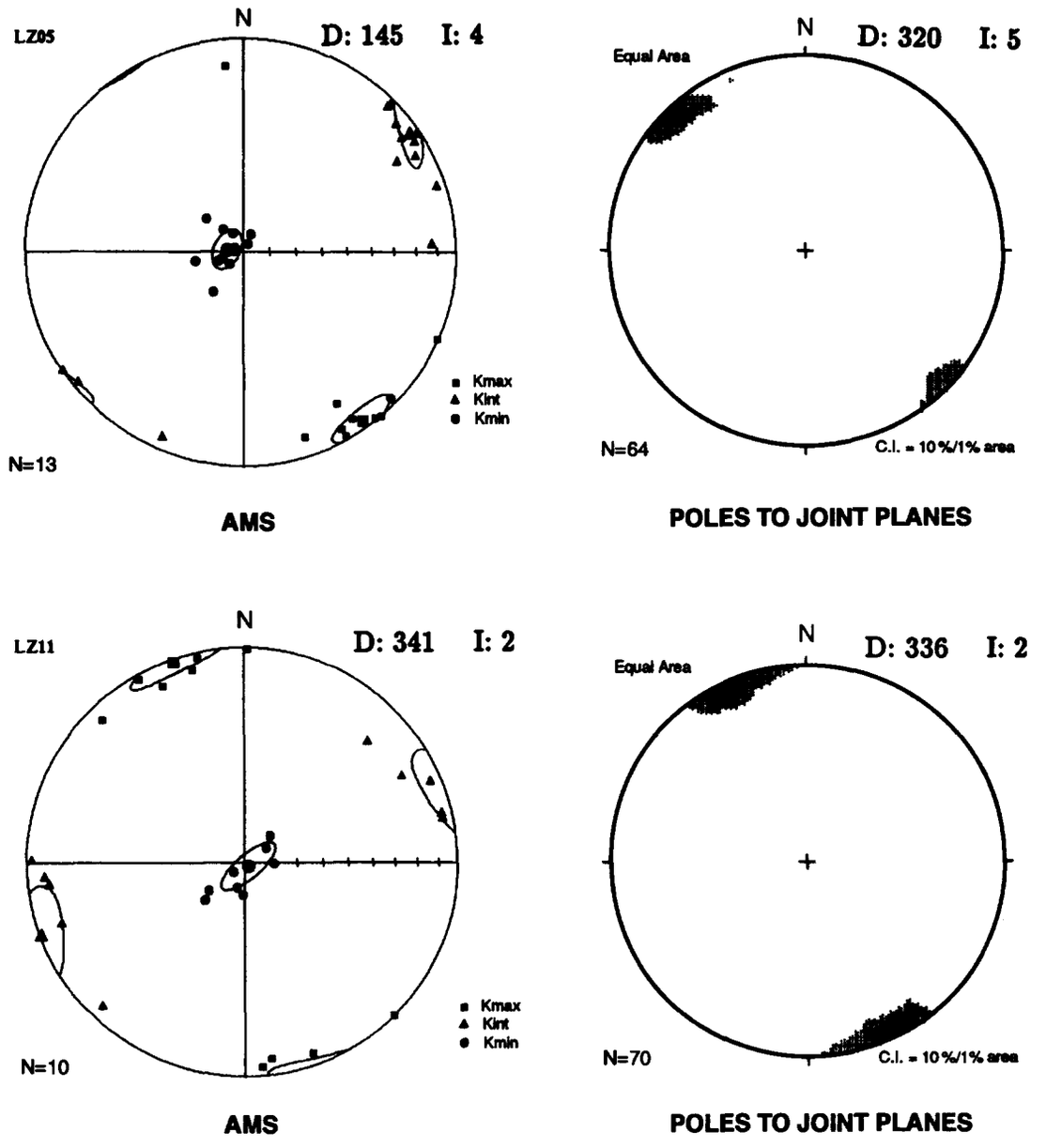

Fig. 14. Magnetic fabrics and structural measurements (only poles to joint planes are shown) at sites LZ05 and LZ11, sampled at two different mining fronts in the UNICEM quarry (Guidonia). Schmidt equal-area projections, lower-hemisphere. The agreement between the two independent analyses at the site scale points to a small difference in the direction of the maximum extension at the two sites (≈N320°–N325° at site LZ05; ≈N335°–N340° at site LZ11).

The first has been recognized at Torre Astura: the mean magnetic ellipsoid is weakly oblate with the k_{min} axes loosely grouped around the vertical and the other two principal axes scattered in the horizontal plane. This fabric can be related to clastic sedimentation, with the flattened grains statistically parallel to the depositional surface.

The second type is characterized by the k_{min} axes tightly clustered around the bedding poles and the other axes scattered in the bedding plane. This fabric, mostly represented at the three sites sampled in Rome, displays no effects of strain but can be related to sediment compaction, resulting in a grouping of the k_{min} axes.

The third type is typical of the very first stages of deformation and it has clear structural evidence in Plio-Pleistocene tectonics. The k_{min} axes are still grouped around the bedding poles but the mean susceptibility ellipsoids are typically triaxial, with a well-defined magnetic lineation parallel to the maximum extensional direction in the bedding planes. This fabric arises from the limited overprinting of a tectonic fabric upon the primary sedimentary-compactional fabric of the undeformed sediments. In the Tiber valley north of Rome, characterized by the presence of right-lateral shear zones, the strain pattern of the Plio-Pleistocene clayey deposits suggests a maximum extensional axis oriented N320°–N330°. Traces of NNW–SSE extension were also found around the Tolfa–Ceriti Mountains. In the Ardea basin the data points to a purely extensional tectonic regime with a maximum extensional axis oriented N310°–N320°.

These data are considered representative of the struc-

tural setting developed from major transverse tectonic features related to the general NE–SW extension of the Tyrrhenian margin. Structural and AMS data indicate that purely extensional mechanisms may occur along such transverse structures, giving rise to peculiar basins, where extension may represent the major agent of the deformation.

Acknowledgements—We are grateful to Fabio Florindo and Fabrizio Marra for the contributions they made at many stages of this research. We express our appreciation to Gary R. Scott for stimulating comments on a previous draft of this paper. The paper also benefited greatly from thorough reviews by Roy Kligfield and Giorgio Minelli.

REFERENCES

Angelier, J. & Gouguel, J. 1979. Sur une methode simple de determination des axes principaux des contraintes pour une population des failles. *C. r. Acad. Sci., Paris* **288**, 307–310.

Averbuch, O., Frizon de Lamotte, D. & Kissel, C. 1992. Magnetic fabric as a structural indicator of the deformation path within a fold-thrust structure: a test case from the Corbières (NE Pyrenees, France). *J. Struct. Geol.* **14**, 461–474.

Averbuch, O. 1993. Characterisation de la déformation dans les structures de chevauchement-plissement. Utilisation couplée du magnétisme des roches et de l'analyse structurale (Examples dans les Corbières, l'Apennin Central et le Taurus Occidental). Unpublished Doctor's degree thesis, University of Paris XI Orsay.

Borradaile, G. J. 1988. Magnetic susceptibility, petrofabrics and strain. *Tectonophysics* **156**, 1–20.

Elter, P., Giglia, G., Tongiorgi, M. & Trevisan, L. 1975, Tensional and compressional areas in the recent (Tortonian to Present) evolution of north Apennines. *Boll. Geof. Teor. Appl.* **17**, 3–18.

Faccenna, C., Funiciello, R. & Mattei, M. In press. Late Pleistocene N–S shear zones along the Latium Tyrrhenian margin: structural characters and volcanological implications. *Boll. Geof. Teor. Appl.*

Funiciello, R., Mattei, M. & Voltaggio, M. 1992. Recent strike slip faulting and problems of possible reactivation in Rome area. In: *Earthquake Prediction* (edited by Boschi, E. & Dragoni, M.). Il Cigno Galilei, Roma, 225–236.

Funiciello, R., Parotto, M. & Praturlon, A. 1981. Carta Tettonica d'Italia 1:1.500.000. C.N.R., Prog. Geodinamica, Publ. 269, Roma.

Graham, J. W. 1966. Significance of magnetic anisotropy in Appalachian sedimentary rocks. In: *The Earth Beneath the Continents* (edited by Steinhart, J. S. & Smith, T. J.). *Am. Geophys. Un. Geophys. Monogr.* **10**, 627–648.

Hrouda, F. 1982. Magnetic anisotropy of rocks and its application in geology and geophysics. *Geophys. Surv.* **5**, 37–82.

Hrouda, F. & Kahan, S. 1991. The magnetic fabric relationship between sedimentary and basement nappes in the High Tatra Mountains, N. Slovakia. *J. Struct. Geol.* **13**, 431–442.

Jackson, M. & Tauxe, L. 1991. Anisotropy of magnetic susceptibility and remanence: developments in the characterization of tectonic, sedimentary and igneous fabric. *Rev. Geophys.* **29**, 371–376.

Jelinek, V. 1977. *The Statistical Theory of Measuring Anisotropy of Magnetic Susceptibility of Rocks and its Applications*. Geofyzika, Brno.

Jelinek, V. 1978. Statistical processing of anisotropy of magnetic susceptibility measured on groups of specimens. *Stud. Geophys. Geod.* **22**, 50–62.

Kissel, C., Barrier, E., Laj, C. & Lee, T. Q. 1986. Magnetic fabric in "undeformed" marine clays from compressional zones. *Tectonics* **5**, 769–781.

Kligfield, R., Lowrie, W. & Dalziel, W. D. 1977. Magnetic susceptibility anisotropy as a strain indicator in the Sudbury Basin, Ontario. *Tectonophysics* **40**, 287–308.

Lee, T. Q., Kissel, C., Laj, C., Horng, C. S. & Lue, Y. T. 1990. Magnetic fabric analysis of the Plio-Pleistocene sedimentary formations of the Coastal Range of Taiwan. *Earth Planet. Sci. Lett.* **98**, 23–32.

Locardi, E., Lombardi, G., Funiciello, R. & Parotto, M. 1977. The main volcanic groups of Latium (Italy): relations between structural evolution and petrogenesis. *Geol. Rom.* **15**, 279–300.

Lowrie, W. & Hirt, A. M. 1987. Anisotropy of magnetic susceptibility in the Scaglia Rossa pelagic limestone. *Earth Planet. Sci. Lett.* **82**, 349–356.

Lowrie, W. 1989. Magnetic analysis of rock fabric. In: *Encyclopedia of Solid Earth Geophysics* (edited by James, D. E.). Van Nostrand Reinhold, New York, 698–706.

Maiorani, A., Funiciello, R., Mattei, M. & Turi, B. 1992. Stable isotope geochemistry and structural elements of the Sabina region (Central Apennines, Italy). *Terra Nova* **4**, 484–488.

Mariani, M. & Prato, R. 1988. I bacini neogenici costieri del margine tirrenico: approccio sismico-stratigrafico. *Mem. Soc. geol. It.* **41**, 519–531.

Patacca, E., Sartori, R. & Scandone, P. 1990. Tyrrhenian Basin and Appenninic Arcs: kinematic relations since late Tortonian times. *Mem. Soc. geol. It.* **45**, 425–451.

Sagnotti, L. & Speranza, F. 1993. Magnetic fabric analysis of the Plio-Pleistocene clayey units of the Sant'Arcangelo basin, Southern Italy. *Phys. Earth & Planet. Interiors* **77**, 165–176.

Turner, G. M. & Gough, D. I. 1983. Magnetic fabric, strain and paleostress in the Canadian Rocky Mountains. *Tectonophysics* **96**, 311–330.